

Dissociation of Large- p_T Prompt J/ψ Produced in Pb-Pb Collisions at the LHC

Shi-Tao Ji¹, Xiao-Ming Xu¹ and H. J. Weber²

¹Department of Physics, Shanghai University, Baoshan, Shanghai 200444, China

²Department of Physics, University of Virginia, Charlottesville, VA 22904, USA

Abstract

A collision of a light meson and a charmonium produces quarks and antiquarks first, then the charm quark fragments into a charmed hadron, and finally three or more mesons are produced. This is the mechanism that we consider and propose to understand the prompt- J/ψ nuclear modification factor in the range of J/ψ transverse momentum from 10 GeV/ c to 18 GeV/ c , as measured by the CMS Collaboration and the ATLAS Collaboration. Unpolarized cross sections are derived and calculated for the reactions $\pi + \text{charmonium} \rightarrow H_c + X$ with H_c being D^+ , D^0 , D_s^+ , D^{*+} , or D^{*0} . Numerical cross sections are parametrized and used to calculate the dissociation rate of charmonium in the interaction with pions in hadronic matter. The momentum dependence of the rate obtained is so as to lead to a decreasing charmonium nuclear modification factor with increasing transverse momentum.

Keywords: Charmonium dissociation, dissociation rate, quark potential model

PACS: 13.75.Lb; 12.39.Jh; 12.39.Pn

1. Introduction

Even though no hadronic meson beam collision experiments are possible, theoretical efforts to understand hadron-charmonium collisions have been made. With the idea that a gluon with an energy larger than the binding energy of a heavy quarkonium breaks the

quarkonium, the short-distance approach [1–3] gives very small hadron-quarkonium cross sections near the threshold energy and increasing cross section at large center-of-mass energy \sqrt{s} of the hadron and the quarkonium. This approach does not specify what are the final hadrons formed in the breakup of the heavy quarkonium.

Through exchange of charmed mesons a light hadron breaks J/ψ . In the meson-exchange approach [4–10] the cross section for any endothermic reaction increases rapidly as \sqrt{s} increases from the threshold energy. Haglin and Gale showed that the $\pi + J/\psi$ ($\rho + J/\psi$) total inelastic cross section would reach an extremely large value of roughly 100 mb (200 mb) at $\sqrt{s} = 6$ GeV. Similar large cross sections have been reported by Oh, Song and Lee. The incorrect magnitude of cross sections comes from pointlike hadron vertices between which the exchange of heavy mesons leads to an interaction too short-ranged to allow the interacting particles to initiate the required J/ψ dissociation reactions. To get reasonable cross sections and to justify the meson-exchange approach, hadronic form factors are inserted in three-meson and four-meson vertices. When the center-of-mass energy of the hadron and J/ψ rises far away from threshold, the increase or decrease of the cross section depends on the choice of the form factors. At present, the meson-exchange approach deals with only 2-to-2 hadron- J/ψ reactions.

We may use quark potential models in the Born approximation to study hadron-charmonium dissociation which is governed by interchange of the quark in the hadron and the charm quark in the charmonium [11–15]. It is concluded in the quark-interchange approach that the dissociation cross section increases rapidly from 0 for an endothermic reaction or decreases rapidly from infinity for an exothermic reaction while \sqrt{s} increases from the threshold energy. No matter which reaction is relevant, endothermic or exothermic, the cross section is very small when \sqrt{s} is larger than the threshold energy plus 1 GeV. Now we raise the question, do the quark potential models really give the very small cross sections at large \sqrt{s} ? The answer is no, but we mention that the quark-interchange mechanism leads to the 2-to-2 hadron-charmonium reactions with the above results. Therefore, we need to think about a new mechanism that provides appreciable hadron-charmonium dissociation cross sections at large \sqrt{s} . This is the subject of the

present work.

Charmonium dissociation causes the nuclear modification of charmonia. The change of the nuclear modification of J/ψ as a function of its transverse momentum p_T is very interesting in relativistic heavy-ion collisions. For nucleus-nucleus collisions at $\sqrt{s_{NN}} = 200$ GeV the prompt- J/ψ transverse momentum measured by the PHENIX Collaboration [16] and the STAR Collaboration [17] is well below 10 GeV/ c . For Pb-Pb collisions at the Large Hadron Collider (LHC) the prompt- J/ψ transverse momentum measured by the CMS Collaboration at $\sqrt{s_{NN}} = 2.76$ TeV [18] and the ATLAS Collaboration at $\sqrt{s_{NN}} = 5.02$ TeV [19] can be beyond 10 GeV/ c . Both data show a suppression pattern of the prompt J/ψ . The p_T dependence of the ATLAS data is that the nuclear modification factor stays unchanged from 10 GeV/ c to 18 GeV/ c and increases slowly from 18 GeV/ c to 40 GeV/ c . The contribution of the nuclear absorption to the nuclear modification factor is expected to be negligible due to the very small $c\bar{c}$ size produced in a parton-parton collision and the very short crossing time of the $c\bar{c}$ pair through colliding nuclei at the LHC. The meson-charmonium dissociation induced by quark interchange in hadronic matter is completely negligible in the suppression of J/ψ with a momentum beyond 10 GeV/ c [20]. Recombination of charm quarks and charm antiquarks in a quark-gluon plasma does not contribute to the nuclear modification factor beyond 10 GeV/ c [21, 22]. The J/ψ nuclear modification at such large transverse momenta are caused by other factors, for example, nuclear parton shadowing in the colliding nuclei [23–25], J/ψ dissociation in collisions with gluons in the quark-gluon plasma [2, 26, 27], decreasing dissociation temperature with increasing J/ψ velocity [28], and radiative energy loss of a gluon traveling through the plasma before gluon fragmentation into a J/ψ meson. Yet, dilating formation time of J/ψ with increasing momentum observed in the plasma rest frame reduces the J/ψ suppression [21]. We denote by R'_{AA} the nuclear modification factor resulting from the above factors together with the formation-time effect. For the J/ψ meson with a momentum larger than 10 GeV/ c , in the present work, we consider that three or more mesons are produced in the collision of a light meson and a charmonium. One of the produced mesons is a charmed meson. We estimate cross sections for $\pi + J/\psi \rightarrow H_c + X$ with H_c being D^+ , D^0 ,

D_s^+ , D^{*+} , or D^{*0} and X representing two or more mesons, and calculate the dissociation rate of J/ψ in the interaction with π in hadronic matter. The J/ψ meson with the momentum 20 GeV/ c has the dissociation rate 0.0108 c/fm at a temperature of 0.95 times the critical temperature T_c . If the lifetime of hadronic matter in longitudinal expansion with a freeze-out temperature of $0.7T_c$ is 5-10 fm/ c , inclusion of the $\pi + J/\psi$ reaction leads to the nuclear modification factor which is 0.973-0.946 times R'_{AA} . Therefore, the meson-charmonium dissociation mechanism proposed here is a source for the J/ψ suppression at momenta beyond 10 GeV/ c . This is in contrast to the quark-interchange mechanism which produces two charmed mesons in meson-charmonium dissociation and works well for low-momentum charmonia [11–15].

In Section 2 the mechanism is given and relevant formulas are presented. In Section 3 we show π -charmonium dissociation cross sections generated by the mechanism and the dissociation rate of the charmonium in the interaction with the pion in hadronic matter. Relevant discussions are given. Section 4 contains the summary.

2. Formulas

We consider the reaction $A(q\bar{q}) + B(c\bar{c}) \rightarrow q + \bar{q} + c + \bar{c} \rightarrow H_c + X$, which means that a collision of meson A and meson B produces quarks and antiquarks (q , \bar{q} , c , and \bar{c}), the charm quark fragments into hadron H_c , and q , \bar{q} , and \bar{c} give rise to two or more mesons. The symbol X actually represents two or more mesons of which one meson contains \bar{c} . The reaction breaks the charmonium, i.e., meson B . The differential cross section for the reaction is

$$d\sigma = \frac{(2\pi)^4 |\mathcal{M}_{\text{fi}}|^2}{4\sqrt{(P_A \cdot P_B)^2 - m_A^2 m_B^2}} \frac{d^3 p'_q}{(2\pi)^3 2E'_q} \frac{d^3 p'_{\bar{q}}}{(2\pi)^3 2E'_{\bar{q}}} \frac{d^3 p'_c}{(2\pi)^3 2E'_c} \frac{d^3 p'_{\bar{c}}}{(2\pi)^3 2E'_{\bar{c}}} \times dz D_c^{H_c}(z, \mu^2) \delta^4(P_A + P_B - p'_q - p'_{\bar{q}} - p'_c - p'_{\bar{c}}), \quad (1)$$

where $p'_i = (E'_i, \vec{p}'_i)$ ($i = q, \bar{q}, c, \bar{c}$) are the four-momenta of q , \bar{q} , c , and \bar{c} ; m_A (m_B) and P_A (P_B) are the mass and four-momentum of meson A (B), respectively; $D_c^{H_c}(z, \mu^2)$ is the $c \rightarrow H_c$ fragmentation function at the factorization scale μ ; z is the fraction of energy passed on from quark c to hadron H_c ; \mathcal{M}_{fi} is the transition amplitude for $A + B \rightarrow$

$q + \bar{q} + c + \bar{c}$.

With the Mandelstam variable $s = (P_A + P_B)^2$, integration over \vec{p}'_q and $|\vec{p}'_q|$ yields

$$d\sigma = \frac{1}{32(2\pi)^8 \sqrt{[s - (m_A + m_B)^2][s - (m_A - m_B)^2]}} d\Omega'_q \frac{d^3 p'_c}{E'_c} \frac{d^3 p'_{\bar{c}}}{E'_{\bar{c}}} \times dz D_c^{H_c}(z, \mu^2) \frac{|\vec{p}'_q|_0^2 |\mathcal{M}_{\text{fi}}|^2}{\left| |\vec{p}'_q|_0 E'_{\bar{q}} + (|\vec{p}'_q|_0 - |\vec{P}_A + \vec{P}_B - \vec{p}'_c - \vec{p}'_{\bar{c}}| \cos \Theta) E'_q \right|}, \quad (2)$$

where Θ is the angle between \vec{p}'_q and $\vec{P}_A + \vec{P}_B - \vec{p}'_c - \vec{p}'_{\bar{c}}$, and $d\Omega'_q$ is the solid angle centered about the direction of \vec{p}'_q . $|\vec{p}'_q|_0$ is determined by the energy conservation,

$$E_A + E_B - E'_q - E'_{\bar{q}} - E'_c - E'_{\bar{c}} = 0, \quad (3)$$

where E_A and E_B are the energies of mesons A and B , respectively.

We calculate the cross section in the center-of-momentum frame of mesons A and B . Denote the maxima of $|\vec{p}'_c|$ and $|\vec{p}'_{\bar{c}}|$ by $p'_{c\text{max}}$ and $p'_{\bar{c}\text{max}}$, respectively. We obtain $p'_{c\text{max}}$ and $p'_{\bar{c}\text{max}}$ by setting $\vec{p}'_q = \vec{p}'_{\bar{q}} = 0$, and they satisfy

$$\sqrt{s} = \sqrt{m_c^2 + p'^2_{c\text{max}}} + \sqrt{m_{\bar{c}}^2 + p'^2_{\bar{c}\text{max}}} + m_q + m_{\bar{q}}, \quad (4)$$

where m_i ($i = q, \bar{q}, c, \bar{c}$) are the masses of $q, \bar{q}, c,$ and \bar{c} . The maxima are

$$p'_{\bar{c}\text{max}} = p'_{c\text{max}} = \frac{1}{2(\sqrt{s} - m_q - m_{\bar{q}})} [(\sqrt{s} - m_q - m_{\bar{q}} - m_c - m_{\bar{c}})(\sqrt{s} - m_q - m_{\bar{q}} + m_c - m_{\bar{c}})(\sqrt{s} - m_q - m_{\bar{q}} - m_c + m_{\bar{c}})(\sqrt{s} - m_q - m_{\bar{q}} + m_c + m_{\bar{c}})]^{\frac{1}{2}}. \quad (5)$$

Denote the minimum of $|\vec{p}'_c|$ by $p'_{c\text{min}}$. The fragmentation of the charm quark into hadron H_c requires $\sqrt{m_c^2 + p'^2_{c\text{min}}} = m_{H_c}$, which gives

$$p'_{c\text{min}} = \sqrt{m_{H_c}^2 - m_c^2}, \quad (6)$$

where m_{H_c} is the mass of hadron H_c .

The cross section for $A(q\bar{q}) + B(c\bar{c}) \rightarrow q + \bar{q} + c + \bar{c} \rightarrow H_c + X$ via $c \rightarrow H_c$ is

$$\sigma(\sqrt{s}, T) = \frac{1}{32(2\pi)^8 \sqrt{[s - (m_A + m_B)^2][s - (m_A - m_B)^2]}} \int d\Omega'_q \int_{p'_{c\text{min}}}^{p'_{c\text{max}}} \frac{d^3 p'_c}{E'_c}$$

$$\begin{aligned}
& \times \int_0^{p'_{c\max}} \frac{d^3 p'_c}{E'_c} \int_{m_{H_c}/E'_c}^1 dz D_c^{H_c}(z, \mu^2) \\
& \times \frac{|\vec{p}'_q|_0^2 |\mathcal{M}_{\text{fi}}|^2}{\left[|\vec{p}'_q|_0 E'_q + (|\vec{p}'_q|_0 - |\vec{P}_A + \vec{P}_B - \vec{p}'_c - \vec{p}'_{\bar{c}}| \cos \Theta) E'_q \right]}. \tag{7}
\end{aligned}$$

In Eq. (7) the transition amplitude is given by

$$\begin{aligned}
\mathcal{M}_{\text{fi}} &= \sqrt{2E_A 2E_B 2E'_q 2E'_{\bar{q}} 2E'_c 2E'_c} \\
& \times \left[V_{q\bar{c}}(\vec{Q}) \psi_A(\vec{p}'_{q\bar{q}} - \frac{m_{\bar{q}}}{m_q + m_{\bar{q}}} \vec{Q}) \psi_B(\vec{p}'_{c\bar{c}} - \frac{m_c}{m_c + m_{\bar{c}}} \vec{Q}) \right. \\
& + V_{\bar{q}c}(\vec{Q}) \psi_A(\vec{p}'_{q\bar{q}} + \frac{m_q}{m_q + m_{\bar{q}}} \vec{Q}) \psi_B(\vec{p}'_{c\bar{c}} + \frac{m_{\bar{c}}}{m_c + m_{\bar{c}}} \vec{Q}) \\
& + V_{qc}(\vec{Q}) \psi_A(\vec{p}'_{q\bar{q}} - \frac{m_{\bar{q}}}{m_q + m_{\bar{q}}} \vec{Q}) \psi_B(\vec{p}'_{c\bar{c}} + \frac{m_{\bar{c}}}{m_c + m_{\bar{c}}} \vec{Q}) \\
& \left. + V_{\bar{q}\bar{c}}(\vec{Q}) \psi_A(\vec{p}'_{q\bar{q}} + \frac{m_q}{m_q + m_{\bar{q}}} \vec{Q}) \psi_B(\vec{p}'_{c\bar{c}} - \frac{m_c}{m_c + m_{\bar{c}}} \vec{Q}) \right], \tag{8}
\end{aligned}$$

where \vec{Q} is the gluon three-dimensional momentum; \vec{p}'_{ij} ($i, j = q, \bar{q}, c, \bar{c}$) is the relative quark momentum; ψ_A (ψ_B) represents the product of color, spin, flavor, and relative-motion wave functions of the quark and antiquark inside meson A (B), and satisfies $\int \frac{d^3 p_{q\bar{q}}}{(2\pi)^3} \psi_A^+(\vec{p}_{q\bar{q}}) \psi_A(\vec{p}_{q\bar{q}}) = \int \frac{d^3 p_{c\bar{c}}}{(2\pi)^3} \psi_B^+(\vec{p}_{c\bar{c}}) \psi_B(\vec{p}_{c\bar{c}}) = 1$, where $\vec{p}_{q\bar{q}}$ ($\vec{p}_{c\bar{c}}$) is the relative momentum of the quark and antiquark inside meson A (B).

The fragmentation functions are solutions of the Dokshitzer-Gribov-Lipatov-Altarelli-Paris (DGLAP) evolution equations [29]. The starting point μ_0 for the DGLAP evolution in the factorization scale μ is taken to be the charm quark mass, i.e., $\mu_0 = m_c$. The charm-quark fragmentation functions at μ_0 are given in Ref. [30] at next-to-leading order in the modified minimal-subtraction factorization scheme by fitting the e^+e^- data taken by the OPAL Collaboration at the CERN Large Electron-Positron Collider:

$$D_c^{D^+}(z, \mu_0^2) = 0.266 \frac{z(1-z)^2}{[(1-z)^2 + 0.108z]^2}, \tag{9}$$

$$D_c^{D^0}(z, \mu_0^2) = 0.781 \frac{z(1-z)^2}{[(1-z)^2 + 0.119z]^2}, \tag{10}$$

$$D_c^{D_s^+}(z, \mu_0^2) = 0.0381 \frac{z(1-z)^2}{[(1-z)^2 + 0.0269z]^2}, \tag{11}$$

$$D_c^{D^{*+}}(z, \mu_0^2) = 0.192 \frac{z(1-z)^2}{[(1-z)^2 + 0.0665z]^2}. \tag{12}$$

As in Ref. [29] we set $\mu = \sqrt{s}$. The fragmentation functions are assumed to be universal and are thus used in hadron-charmonium reactions.

Denote the orbital angular momentum and the spin of meson A (B) by L_A (L_B) and S_A (S_B), respectively. Let L_{Bz} be the magnetic projection quantum number of L_B . The unpolarized cross section is

$$\sigma^{\text{unpol}}(\sqrt{s}, T) = \frac{1}{(2S_A + 1)(2S_B + 1)(2L_B + 1)} \sum_{L_{Bz} S S_{q+\bar{q}} S_{c+\bar{c}}} (2S + 1) \sigma(\sqrt{s}, T), \quad (13)$$

which holds true for the three cases: $L_A = 0, L_B = 0$; $L_A = 0, L_B \neq 0, S_A = 0$; $L_A = 0, L_B = 1, S_A = 1, S_B = 1$. The total spin S of mesons A and B satisfies $|S_A - S_B| \leq S \leq S_A + S_B$ and $|S_{q+\bar{q}} - S_{c+\bar{c}}| \leq S \leq |S_{q+\bar{q}} + S_{c+\bar{c}}|$, where $S_{q+\bar{q}}$ ($S_{c+\bar{c}}$) is the total spin of q and \bar{q} (c and \bar{c}).

The potential V_{ab} used in the transition amplitude is the Fourier transform of the following potential in coordinate space [14],

$$V_{ab}(\vec{r}) = V_{\text{si}}(\vec{r}) + V_{\text{ss}}(\vec{r}), \quad (14)$$

where \vec{r} is the relative coordinate of constituents a and b , V_{si} the central spin-independent potential, and V_{ss} the spin-spin interaction. The spin-independent potential depends on temperature T and below the critical temperature $T_c = 0.175$ GeV is given by

$$V_{\text{si}}(\vec{r}) = -\frac{\vec{\lambda}_a}{2} \cdot \frac{\vec{\lambda}_b}{2} \frac{3}{4} D \left[1.3 - \left(\frac{T}{T_c} \right)^4 \right] \tanh(Ar) + \frac{\vec{\lambda}_a}{2} \cdot \frac{\vec{\lambda}_b}{2} \frac{6\pi}{25} \frac{v(\lambda r)}{r} \exp(-Er), \quad (15)$$

where $D = 0.7$ GeV, $A = 1.5[0.75 + 0.25(T/T_c)^{10}]^6$ GeV, $E = 0.6$ GeV, and $\lambda = \sqrt{3b_0/16\pi^2\alpha'}$ in which $\alpha' = 1.04$ GeV⁻² and $b_0 = 11 - \frac{2}{3}N_f$ with the quark flavor number $N_f = 4$. $\vec{\lambda}_a$ are the Gell-Mann matrices for the color generators of constituent quark or antiquark labeled as a . The dimensionless function $v(x)$ is given by Buchmüller and Tye [31]. The short-distance part of the spin-independent potential originates from one-gluon exchange plus perturbative one- and two-loop corrections. The intermediate-distance and large-distance part of the spin-independent potential fits well the numerical potential which was obtained in the lattice gauge calculations [32] and was assumed to be the free energy. At large distances the spin-independent potential is independent of the relative

coordinate and obviously exhibits a plateau at $T/T_c > 0.55$. The plateau height decreases with increasing temperature. This means that confinement becomes weaker and weaker.

In this paragraph we mention six references which show that the quark-antiquark free energy can not be taken as the quark-antiquark potential when the temperature is above the critical temperature. The quark-antiquark free energy $F_{Q\bar{Q}}$ is defined as the quark-antiquark internal energy $U_{Q\bar{Q}}$ minus the product of the temperature and the quark-antiquark entropy $S_{Q\bar{Q}}$. The internal energy of a quark and an antiquark at rest is the quark-antiquark potential. The free energy of a heavy quark-antiquark pair is related to the Polyakov loop correlation functions and can be obtained from lattice gauge calculations. It is real! Since the lattice calculations provide the internal energy $U(T, r)$ that includes the internal energy of the heavy quark-antiquark pair and the gluon internal energy difference $U_g(T, r) - U_{g0}(T)$ where $U_g(T, r)$ and $U_{g0}(T)$ correspond to the gluon internal energies in the presence and the absence of the heavy quark-antiquark pair, respectively, it was proposed by Wong [33] that the heavy quark-antiquark potential should be $U(T, r) - [U_g(T, r) - U_{g0}(T)]$ and may be taken as a linear combination of $F_{Q\bar{Q}}$ and $U(T, r)$. Authors in Ref. [34] have derived a static quark-antiquark potential in a deconfined medium by defining a suitable gauge-invariant Green's function and computing it to first non-trivial order in Hard Thermal Loop resummed perturbation theory. The potential consists of a real part and an imaginary part. Authors in Ref. [35] have also derived a static quark-antiquark potential in the deconfined medium in potential nonrelativistic QCD. The potential has various expressions that depend on the relation among the temperature, the Debye mass, and the inverse of the quark-antiquark distance. Authors in Refs. [36–38] have obtained a quark-antiquark potential from the spectral function of the thermal Wilson loop in Coulomb gauge in dynamical lattice QCD with u , d , and s flavors. The imaginary part of the potential is comparable with the result of the Hard Thermal Loop resummed perturbation theory.

In this paragraph we mention two references which show that the quark-antiquark free energy can be taken as the quark-antiquark potential when the temperature is above the critical temperature. Using the free energy from lattice calculations as the potential

of a charm quark and a charm antiquark in the Schrödinger equation correctly describes the nonrelativistic J/ψ wave function and reproduces the J/ψ mass from the QCD sum rule in the vicinity of the critical temperature [39]. The entropic force is the derivative of the entropy with respect to the quark-antiquark distance when the temperature is fixed. The stronger increase of the internal energy with increasing quark-antiquark distance is compensated by an equally strong contribution from the repulsive entropic force. Thus, it is suggested by Satz that the potential is the free energy [40].

In this paragraph we indicate that the quark-antiquark free energy can be taken as the quark-antiquark potential when the temperature is below the critical temperature. Let the quark-antiquark potential obtained from the spectral function of the thermal Wilson loop be compared to the quark-antiquark free energy. It has been realized that the real part of the potential is close to the free energy at $T < T_c$ and the imaginary part is negligible [36, 37, 41, 42]. In hadronic matter $TS_{Q\bar{Q}}$ is quite small in comparison with the free energy, and the quark-antiquark internal energy, i.e., the potential, then approximately equals the free energy [43].

Denote by \vec{s}_a the spin of constituent a . The spin-spin interaction with relativistic effects [44, 45] is [14, 46]

$$V_{ss}(\vec{r}) = -\frac{\vec{\lambda}_a}{2} \cdot \frac{\vec{\lambda}_b}{2} \frac{16\pi^2}{25} \frac{d^3}{\pi^{3/2}} \exp(-d^2 r^2) \frac{\vec{s}_a \cdot \vec{s}_b}{m_a m_b} + \frac{\vec{\lambda}_a}{2} \cdot \frac{\vec{\lambda}_b}{2} \frac{4\pi}{25} \frac{1}{r} \frac{d^2 v(\lambda r)}{dr^2} \frac{\vec{s}_a \cdot \vec{s}_b}{m_a m_b}, \quad (16)$$

of which the flavor dependence is relevant to quark masses as shown in $1/m_a m_b$ and d ,

$$d^2 = \sigma_0^2 \left[\frac{1}{2} + \frac{1}{2} \left(\frac{4m_a m_b}{(m_a + m_b)^2} \right)^4 \right] + \sigma_1^2 \left(\frac{2m_a m_b}{m_a + m_b} \right)^2, \quad (17)$$

where $\sigma_0 = 0.15$ GeV and $\sigma_1 = 0.705$.

Solving the Schrödinger equation with the central spin-independent potential plus the spin-spin interaction, we obtain meson masses and quark-antiquark relative-motion wave functions with the charm-quark mass, the up-quark mass, and the strange-quark mass being 1.51 GeV, 0.32 GeV, and 0.5 GeV, respectively. The experimental masses of π , ρ , K , K^* , η , ϕ , J/ψ , ψ' , χ_c , D , D^* , D_s , and D_s^* mesons [47] and the experimental data of S -wave $I = 2$ elastic phase shifts for $\pi\pi$ scattering in vacuum [48] are reproduced with $V_{ab}(\vec{r})$ at $T = 0$ and the quark-antiquark relative-motion wave functions.

In the mechanism shown above we assume that the interactions among q , \bar{q} , c , and \bar{c} are neglected, and the fragmentation of the charm quark into hadrons is related to quark-antiquark pairs created from the color field around the charm quark, which is similar to the scenario of Feynman and Field [49]. We do not address how the mesons represented by X are formed, and also neglect any temperature dependence of the fragmentation.

3. Numerical results and discussions

We consider the charmonium dissociation $\pi + J/\psi \rightarrow H_c + X$, $\pi + \psi' \rightarrow H_c + X$, and $\pi + \chi_c \rightarrow H_c + X$ with $H_c = D^+$, D^0 , D_s^+ , D^{*+} , or D^{*0} . This amounts to 15 reaction channels. We solve the Schrödinger equation with the potential in Eq. (14) to get temperature-dependent quark-antiquark relative-motion wave functions of π , J/ψ , ψ' , and χ_c , calculate the transition amplitude with the wave functions and the potential, and obtain unpolarized cross sections from the transition amplitude and the charm-quark fragmentation functions provided in Ref. [30]. The unpolarized cross sections for $\pi + J/\psi \rightarrow H_c + X$ at the temperatures $T/T_c = 0, 0.65, 0.75, 0.85, 0.9, \text{ and } 0.95$ are shown in Figs. 1-4. Because the D^{*0} fragmentation function is unknown, we assume that it is the same as the D^{*+} fragmentation function. The cross section for $\pi + J/\psi \rightarrow D^{*0} + X$ then equals the cross section for $\pi + J/\psi \rightarrow D^{*+} + X$ and is not shown.

All the reactions are endothermic as shown in Figs. 1-4. When the difference between \sqrt{s} and the threshold energy is less than 1 GeV, the unpolarized cross section is negligible. With increasing \sqrt{s} the cross section increases slowly. At a given temperature and difference between \sqrt{s} and the threshold energy, the cross section for the production of D^0 is largest, the cross section for the production of D_s^+ is smallest, and the cross section for $\pi + \psi' \rightarrow H_c + X$ or $\pi + \chi_c \rightarrow H_c + X$ is larger than the one for $\pi + J/\psi \rightarrow H_c + X$. Since the cross-section curves for $\pi + \psi' \rightarrow H_c + X$ and $\pi + \chi_c \rightarrow H_c + X$ look similar to the ones for $\pi + J/\psi \rightarrow H_c + X$, the former are not shown here.

In Eq. (7) the integration over $|\vec{p}'_c|$ ($|\vec{p}'_{\bar{c}}|$) has the lower limit $p'_{c\min}$ (0) and the upper limit $p'_{c\max}$ ($p'_{\bar{c}\max}$). $p'_{c\min}$ given in Eq. (6) is independent of \sqrt{s} . While \sqrt{s} increases, $p'_{c\max}$ and $p'_{\bar{c}\max}$ given in Eq. (5) increase. Hence, the phase space of the

produced charm quark and the produced charm antiquark in $A + B \rightarrow q + \bar{q} + c + \bar{c}$ becomes larger and larger. While \sqrt{s} increases, $\sqrt{E_A E_B}$ in Eq. (8) also increases, but the factor $1/\sqrt{[s - (m_A + m_B)^2][s - (m_A - m_B)^2]}$ in Eq. (7) decreases. Therefore, while \sqrt{s} increases from the threshold energy, the cross section increases first, then reaches a maximum, and eventually decreases slowly.

In vacuum the central spin-independent potential is given by the Buchmüller-Tye potential,

$$V_{\text{BT}}(\vec{r}) = -\frac{\vec{\lambda}_a}{2} \cdot \frac{\vec{\lambda}_b}{2} \frac{3}{4} kr + \frac{\vec{\lambda}_a}{2} \cdot \frac{\vec{\lambda}_b}{2} \frac{6\pi}{25} \frac{v(\lambda r)}{r}, \quad (18)$$

with $k = 1/(2\pi\alpha')$. The quark potential in vacuum is

$$V_{\text{vac}}(\vec{r}) = V_{\text{BT}}(\vec{r}) + V_{\text{ss}}(\vec{r}). \quad (19)$$

Using the potential $V_{\text{vac}}(\vec{r})$ in the transition amplitude, we get numerical unpolarized cross sections by Eq. (13). Dotted curves in Fig. 8 show the cross sections for $\pi + J/\psi \rightarrow H_c + X$ which are compared with the solid curves that stand for the unpolarized cross sections corresponding to the potential in Eq. (14) at $T = 0$. The four solid curves in Fig. 8 are actually the four solid curves in Figs. 1-4. The dotted curves are quite close to the solid curves. The situation is similar with respect to the cross sections for $\pi + \psi' \rightarrow H_c + X$ and $\pi + \chi_c \rightarrow H_c + X$, which are not shown. Thus, the cross sections corresponding to the quark potential in vacuum are quite close to the ones corresponding to the potential in Eq. (14) at $T = 0$. Combining Fig. 8 with Figs. 1-4, every cross-section curve at a nonzero temperature in Figs. 1-4 should intersect a dotted curve in Fig. 8 at a value of \sqrt{s} . Below this value the cross section related to Eq. (14) is larger than the cross section related to Eq. (19) while above this value the former is smaller than the latter. At $\sqrt{s} = 7$ GeV (11 GeV) the cross section for $\pi + J/\psi \rightarrow D^+ + X$, $\pi + J/\psi \rightarrow D^0 + X$, $\pi + J/\psi \rightarrow D_s^+ + X$, and $\pi + J/\psi \rightarrow D^{*+} + X$ at $T/T_c = 0.95$ is 1.97, 1.94, 1.54, and 3.17 (0.77, 0.79, 0.68, and 0.75) times the cross section corresponding to the quark potential in vacuum, respectively. The medium effect on the reactions is obvious at $T/T_c = 0.95$.

A cross section of about 1 mb for $\pi + J/\psi$ dissociation at $\sqrt{s} = 10$ GeV was obtained in the short-distance approach [3]. The usual monopole form with a cutoff parameter

is taken as the form factor inserted in three-meson vertices, and the product of two monopole forms is taken as the form factor inserted in four-meson vertices in the meson-exchange approach. Starting from an effective meson Lagrangian, a cross section of about 3.6 mb for $\pi + J/\psi$ dissociation at $\sqrt{s} = 5$ GeV is given in Ref. [6] with the cutoff parameter 1 GeV. Adding anomalous parity terms to the Lagrangian, a cross section of about 6.4 mb at $\sqrt{s} = 5$ GeV is given in Ref. [7]. While mesonic form factors were calculated from the underlying quark structure, J/ψ dissociation in collisions with π and ρ mesons were studied in Ref. [10] in an extended Nambu-Jona-Lasinio model. The $\pi + J/\psi$ dissociation cross section has a peak value of about 0.83 mb near the threshold energy of $\pi + J/\psi$ dissociation. In the quark-interchange mechanism and in the quark model that possesses the color Coulomb, spin-spin hyperfine, and linear confining interactions, the cross section obtained in Ref. [13] has a peak value of 1.41 mb near threshold. The five values (1 mb, 3.6 mb, 6.4 mb, 0.83 mb, and 1.41 mb) characterize the $\pi + J/\psi$ dissociation cross sections obtained in the short-distance approach, in the meson-exchange approach, and in the quark-interchange approach. In the present work the cross section for $\pi J/\psi \rightarrow D^+ X + D^0 X + D_s^+ X + D^{*+} X + D^{*0} X$ is, for example, 1.46 mb at $\sqrt{s} = 10$ GeV corresponding to the potential in Eq. (14) at $T = 0$, or 1.49 mb corresponding to the potential in Eq. (19). The two values, 1.46 mb and 1.49 mb, are comparable to the above five values. Therefore, the cross section for $\pi + J/\psi$ dissociation due to the present mechanism is not very small at large \sqrt{s} , but depends on the selection among quark potential models.

For the convenient use of the unpolarized cross sections shown in Figs. 1-4, they are parametrized as

$$\begin{aligned} \sigma^{\text{unpol}}(\sqrt{s}, T) = & a_1 \left(\frac{\sqrt{s} - \sqrt{s_0}}{b_1} \right)^{c_1} \exp \left[c_1 \left(1 - \frac{\sqrt{s} - \sqrt{s_0}}{b_1} \right) \right] \\ & + a_2 \left(\frac{\sqrt{s} - \sqrt{s_0}}{b_2} \right)^{c_2} \exp \left[c_2 \left(1 - \frac{\sqrt{s} - \sqrt{s_0}}{b_2} \right) \right], \end{aligned} \quad (20)$$

where $\sqrt{s_0}$ is the threshold energy and equals the sum of the H_c mass, the \bar{D} mass, and 2 times the up-quark mass. The values of the parameters, a_1 , b_1 , c_1 , a_2 , b_2 , and c_2 , are listed in Tables 1-3. The parametrization as a function of \sqrt{s} at a given temperature

has a peak. In the three tables we also give the quantities d_0 and $\sqrt{s_z}$, where d_0 is the separation between the peak's location on the \sqrt{s} -axis and the threshold energy, and $\sqrt{s_z}$ is the square root of the Mandelstam variable at which the cross section is 1/100 of the peak cross section. We note that Eq. (20) is valid for $\sqrt{s_0} \leq \sqrt{s} \leq 11$ GeV.

Having obtained the unpolarized cross sections for the 15 reaction channels, we need to evaluate their influence on the charmonium nuclear modification factor. We thus calculate the dissociation rate of charmonium in the interaction with a pion in hadronic matter,

$$n_\pi \langle v_{\text{rel}} \sigma^{\text{unpol}} \rangle = \frac{3}{4\pi^2} \int_0^\infty \int_{-1}^1 d|\vec{k}| d \cos \theta k^2 v_{\text{rel}} \sigma^{\text{unpol}} f(\vec{k}), \quad (21)$$

where n_π is the π number density, v_{rel} is the relative velocity of the pion and the charmonium, θ is the angle between the π momentum \vec{k} and the charmonium momentum, $f(\vec{k})$ is the Bose-Einstein distribution that pions obey, and the thermal average $\langle v_{\text{rel}} \sigma^{\text{unpol}} \rangle$ is obtained from $f(\vec{k})$ [15]. The dissociation rates are plotted in Figs. 5-7 as functions of charmonium momentum. The rate shown in Fig. 5 is obtained from the sum of the cross sections for $\pi + J/\psi \rightarrow D^+ + X$, $\pi + J/\psi \rightarrow D^0 + X$, $\pi + J/\psi \rightarrow D_s^+ + X$, $\pi + J/\psi \rightarrow D^{*+} + X$, and $\pi + J/\psi \rightarrow D^{*0} + X$. The rate shown in Fig. 6 (7) is obtained from the cross section for $\pi \psi' \rightarrow D^+ X + D^0 X + D_s^+ X + D^{*+} X + D^{*0} X$ ($\pi \chi_c \rightarrow D^+ X + D^0 X + D_s^+ X + D^{*+} X + D^{*0} X$). Given a charmonium momentum the rate increases with increasing temperature. Given a temperature the rate increases with increasing charmonium momentum. At $T/T_c = 0.95$ the rate is about 0.0108 c/fm, 0.0142 c/fm, and 0.0149 c/fm for the $\pi + J/\psi$, $\pi + \psi'$, and $\pi + \chi_c$ reactions, respectively, when the charmonium momentum is 20 GeV/c. Because the nuclear modification factor is the inverse of the exponential function of the dissociation rate [46], the reactions give a decreasing charmonium nuclear modification factor with increasing transverse momentum. This is in sharp contrast with the increasing nuclear modification factor due to nuclear shadowing. Decreasing nuclear modification factors are also caused by other factors, for example, decreasing dissociation temperature with increasing J/ψ velocity [28] and radiative energy loss of a gluon before gluon fragmentation into a J/ψ meson.

The relative velocity depends on the pion and charmonium masses. Since the ψ' mass

is very close to the χ_c mass for $0.6 \leq T/T_c < 1$ [14], the relative velocity of π and ψ' is almost the same as the one of π and χ_c . The cross sections for $\pi + \psi' \rightarrow D^+ + X$, $\pi + \psi' \rightarrow D^0 + X$, $\pi + \psi' \rightarrow D_s^+ + X$, $\pi + \psi' \rightarrow D^{*+} + X$, and $\pi + \psi' \rightarrow D^{*0} + X$ are close to those for $\pi + \chi_c \rightarrow D^+ + X$, $\pi + \chi_c \rightarrow D^0 + X$, $\pi + \chi_c \rightarrow D_s^+ + X$, $\pi + \chi_c \rightarrow D^{*+} + X$, and $\pi + \chi_c \rightarrow D^{*0} + X$, respectively. To account for this, in Table 4 we show the ratio of the difference of the cross section for $\pi + \psi' \rightarrow D^+ + X$ ($\pi + \psi' \rightarrow D^0 + X$, $\pi + \psi' \rightarrow D_s^+ + X$, $\pi + \psi' \rightarrow D^{*+} + X$, $\pi + \psi' \rightarrow D^{*0} + X$) and the one for $\pi + \chi_c \rightarrow D^+ + X$ ($\pi + \chi_c \rightarrow D^0 + X$, $\pi + \chi_c \rightarrow D_s^+ + X$, $\pi + \chi_c \rightarrow D^{*+} + X$, $\pi + \chi_c \rightarrow D^{*0} + X$) at $\sqrt{s} = 9$ GeV to the former. The absolute values of the ratios are less than 0.25 or even close to 0. According to Eq. (21), the dissociation rate of ψ' in the interaction with the pion is similar to the dissociation rate of χ_c .

The meson masses and quark-antiquark relative-motion wave functions determined by the Schrödinger equation with the potential in Eq. (14) depend on temperature. Consequently, p'_{cmin} given in Eq. (6), $|\vec{p}'_q|_0$ determined by Eq. (3), and the transition amplitude \mathcal{M}_{fi} depend on temperature. The cross section given by Eq. (7) may not result in a monotonously increasing or decreasing function of temperature. However, the dissociation rate at a given \sqrt{s} is a monotonously increasing function of temperature. The reason is as follows. With increasing temperature the meson masses decrease [14], the pion distribution function thus increases, and the relative velocity of the pion and the charmonium increases as well. Because the dissociation rate is proportional to the relative velocity and the pion distribution function, the rate increases with increasing temperature.

The potential in Eq. (14) is valid at $T < T_c$. Solving the Schrödinger equation with the potential, we find that J/ψ , ψ' , $\chi_c(1P)$, and $\chi_c(2P)$ are not dissolved in hadronic matter. Similar to Refs. [31] and [45], the experimentally observed states, $\psi(4160)$ and $\psi(4415)$, can be individually interpreted as the 3^3S_1 and 4^3S_1 states that satisfy the Schrödinger equation. When the temperature is larger than $0.97T_c$ and $0.87T_c$, respectively, $\psi(4160)$ and $\psi(4415)$ are dissolved.

4. Summary

We have presented a mechanism for large-momentum charmonium dissociation. In this mechanism the collision between a light meson and a charmonium produces two quarks and two antiquarks; the charm quark fragments into a charmed meson, and the other three constituents give rise to two or more mesons. The cross section for the reaction obeying the mechanism is derived from the transition amplitude and is calculated from the temperature-dependent quark potential. The temperature dependence of the potential, the meson masses, and the mesonic quark-antiquark relative-motion wave functions lead to the temperature dependence of the cross section. From the cross section the dissociation rate of charmonium in the interaction with pions increases with increasing temperature and/or increasing charmonium momentum, and reaches 0.0108 c/fm , 0.0142 c/fm , and 0.0149 c/fm for the $\pi + J/\psi$, $\pi + \psi'$, and $\pi + \chi_c$ reactions, respectively, at $T/T_c = 0.95$ and at the momentum 20 GeV/ c . These rates are small, but already non-negligible. In future work we will include collisions of charmonia with K, η, ρ, K^* and ϕ mesons. The mechanism for large-momentum charmonium dissociation is in contrast to the quark-interchange mechanism for low-momentum charmonium dissociation. The decreasing nuclear modification factor of the prompt J/ψ with increasing momentum is caused not only by $\pi J/\psi \rightarrow D^+X + D^0X + D_s^+X + D^{*+}X + D^{*0}X$, but also by other factors, for example, decreasing dissociation temperature with increasing J/ψ velocity [28] and radiative energy loss of a gluon before gluon fragmentation into a J/ψ meson.

Acknowledgements

We thank anonymous referees whose comments led us to improve our work substantially. This work was supported by the National Natural Science Foundation of China under Grant No. 11175111.

References

- [1] M. E. Peskin, Nucl. Phys. B **156**, 365 (1979); G. Bhanot and M. E. Peskin, Nucl. Phys. B **156**, 391 (1979).
- [2] D. Kharzeev and H. Satz, Phys. Lett. B **334**, 155 (1994).
- [3] F. Arleo, P. B. Gossiaux, T. Gousset, and J. Aichelin, Phys. Rev. D **65**, 014005 (2001).
- [4] S. G. Matinyan and B. Müller, Phys. Rev. C **58**, 2994 (1998).
- [5] K. L. Haglin and C. Gale, Phys. Rev. C **63**, 065201 (2001).
- [6] Z. Lin and C. M. Ko, Phys. Rev. C **62**, 034903 (2000).
- [7] Y. S. Oh, T. S. Song, and S. H. Lee, Phys. Rev. C **63**, 034901 (2001).
- [8] F. S. Navarra, M. Nielsen, and M. R. Robilotta, Phys. Rev. C **64**, 021901(R) (2001).
- [9] L. Maiani, F. Piccinini, A. D. Polosa, and V. Riquer, Nucl. Phys. A **741**, 273 (2004).
- [10] A. Bourque and C. Gale, Phys. Rev. C **80**, 015204 (2009).
- [11] K. Martins, D. Blaschke, and E. Quack, Phys. Rev. C **51**, 2723 (1995).
- [12] C.-Y. Wong, E. S. Swanson, and T. Barnes, Phys. Rev. C **65**, 014903 (2001).
- [13] T. Barnes, E. S. Swanson, C.-Y. Wong, and X.-M. Xu, Phys. Rev. C **68**, 014903 (2003).
- [14] J. Zhou and X.-M. Xu, Phys. Rev. C **85**, 064904 (2012).
- [15] S.-T. Ji, Z.-Y. Shen, and X.-M. Xu, J. Phys. G **42**, 095110 (2015).
- [16] A. Adare et al. (PHENIX Collaboration), Phys. Rev. Lett. **98**, 232301 (2007); Phys. Rev. Lett. **101**, 122301 (2008); Phys. Rev. C **84**, 054912 (2011).

- [17] B. I. Abelev et al. (STAR Collaboration), Phys. Rev. C 80, 041902 (2009); L. Adamczyk et al. (STAR Collaboration), Phys. Lett. B 722, 55 (2013); Phys. Rev. C 90, 024906 (2014).
- [18] S. Chatrchyan et al. (CMS Collaboration), JHEP 05, 063 (2012); P. Shukla, for the CMS Collaboration, arXiv:1405.3810, talk given at International Conference on Matter at Extreme Conditions, 15-17 January 2014, Kolkata, India.
- [19] S. T. Araya, for the ATLAS Collaboration, talk given at the 8th International Conference on Hard and Electromagnetic Probes of High-Energy Nuclear Collisions, 23-27 September 2016, Wuhan, China.
- [20] F.-R. Liu, S.-T. Ji, and X.-M. Xu, J. Korean Phys. Soc. 69, 472 (2016).
- [21] X.-M. Xu, Nucl. Phys. A 658, 165 (1999).
- [22] X. Du and R. Rapp, Nucl. Phys. A 943, 147 (2015).
- [23] M. Arneodo, Phys. Rep. 240, 301 (1994).
- [24] K. J. Eskola, V. J. Kolhinen, and C. A. Salgado, Eur. Phys. J. C 9, 61 (1999); K. J. Eskola, V. J. Kolhinen, and P. V. Ruuskanen, hep-ph/9802350.
- [25] S.-Y. Li and X.-N. Wang, Phys. Lett. B 527, 85 (2002).
- [26] X.-M. Xu, D. Kharzeev, H. Satz, and X.-N. Wang, Phys. Rev. C 53, 3051 (1996).
- [27] K. Zhou, N. Xu, Z. Xu, and P. Zhuang, Phys. Rev. C 89, 054911 (2014).
- [28] H. Liu, K. Rajagopal, and U. A. Wiedemann, Phys. Rev. Lett. 98, 182301 (2007).
- [29] T. Kneesch, B. A. Kniehl, G. Kramer, and I. Schienbein, Nucl. Phys. B 799, 34 (2008).
- [30] B. A. Kniehl and G. Kramer, Phys. Rev. D 74, 037502 (2006).
- [31] W. Buchmüller and S.-H. H. Tye, Phys. Rev. D 24, 132 (1981).

- [32] F. Karsch, E. Laermann, and A. Peikert, Nucl. Phys. B 605, 579 (2001).
- [33] C.-Y. Wong, Phys. Rev. C 72, 034906 (2005).
- [34] M. Laine, O. Philipsen, M. Tassler, and P. Romatschke, JHEP 03, 054 (2007).
- [35] N. Brambilla, J. Ghiglieri, A. Vairo, and P. Petreczky, Phys. Rev. D 78, 014017 (2008).
- [36] Y. Burnier, O. Kaczmarek, and A. Rothkopf, arXiv:1410.7311.
- [37] Y. Burnier, O. Kaczmarek, and A. Rothkopf, JHEP 12, 101 (2015).
- [38] A. Bazavov, Y. Burnier, and P. Petreczky, Nucl. Phys. A 932, 117 (2014).
- [39] S. H. Lee, K. Morita, T. Song, and C. M. Ko, Phys. Rev. D 89, 094015 (2014).
- [40] H. Satz, Eur. Phys. J. C 75, 193 (2015).
- [41] A. Rothkopf, T. Hatsuda, and S. Sasaki, Phys. Rev. Lett. 108, 162001 (2012); Y. Burnier and A. Rothkopf, Phys. Rev. Lett. 111, 182003 (2013).
- [42] Y. Burnier and A. Rothkopf, arXiv:1607.04049.
- [43] Z.-Y. Shen and X.-M. Xu, Chin. Phys. C 39, 074103 (2015).
- [44] T. Barnes and E. S. Swanson, Phys. Rev. D 46, 131 (1992); E. S. Swanson, Ann. Phys. (N.Y.) 220, 73 (1992).
- [45] S. Godfrey and N. Isgur, Phys. Rev. D 32, 189 (1985).
- [46] X.-M. Xu, Nucl. Phys. A 697, 825 (2002).
- [47] J. Beringer et al., Phys. Rev. D 86, 010001 (2012).
- [48] E. Colton et al., Phys. Rev. D 3, 2028 (1971); N. B. Durusoy et al., Phys. Lett. B 45, 517 (1973); W. Hoogland et al., Nucl. Phys. B 126, 109 (1977); M. J. Losty et al., Nucl. Phys. B 69, 185 (1974).
- [49] R. D. Field and R. P. Feynman, Nucl. Phys. B136, 1 (1978).

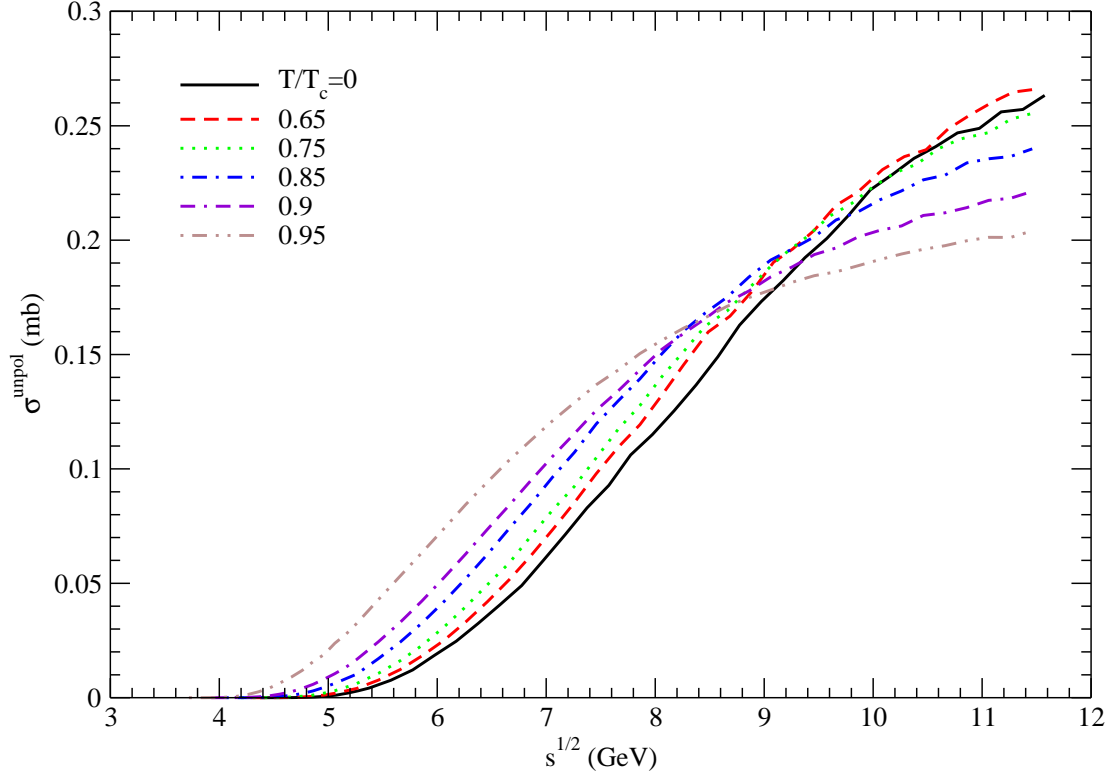


Figure 1: Cross sections for $\pi + J/\psi \rightarrow D^+ + X$ at various temperatures.

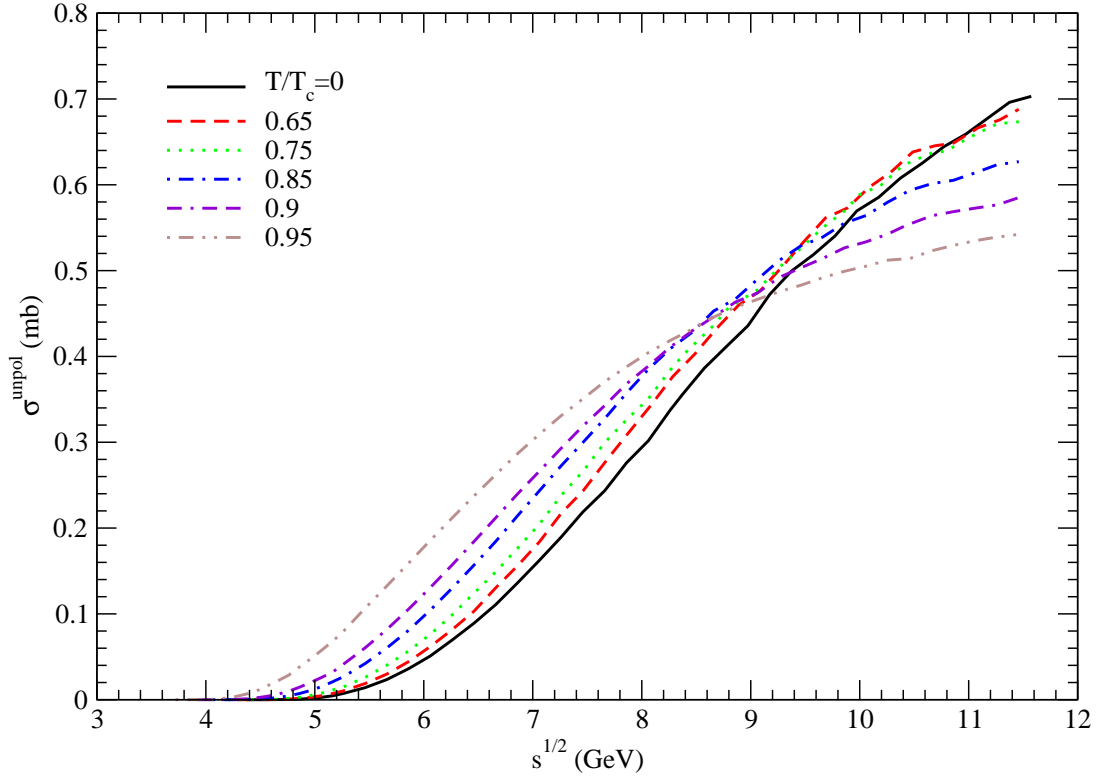


Figure 2: Cross sections for $\pi + J/\psi \rightarrow D^0 + X$ at various temperatures.

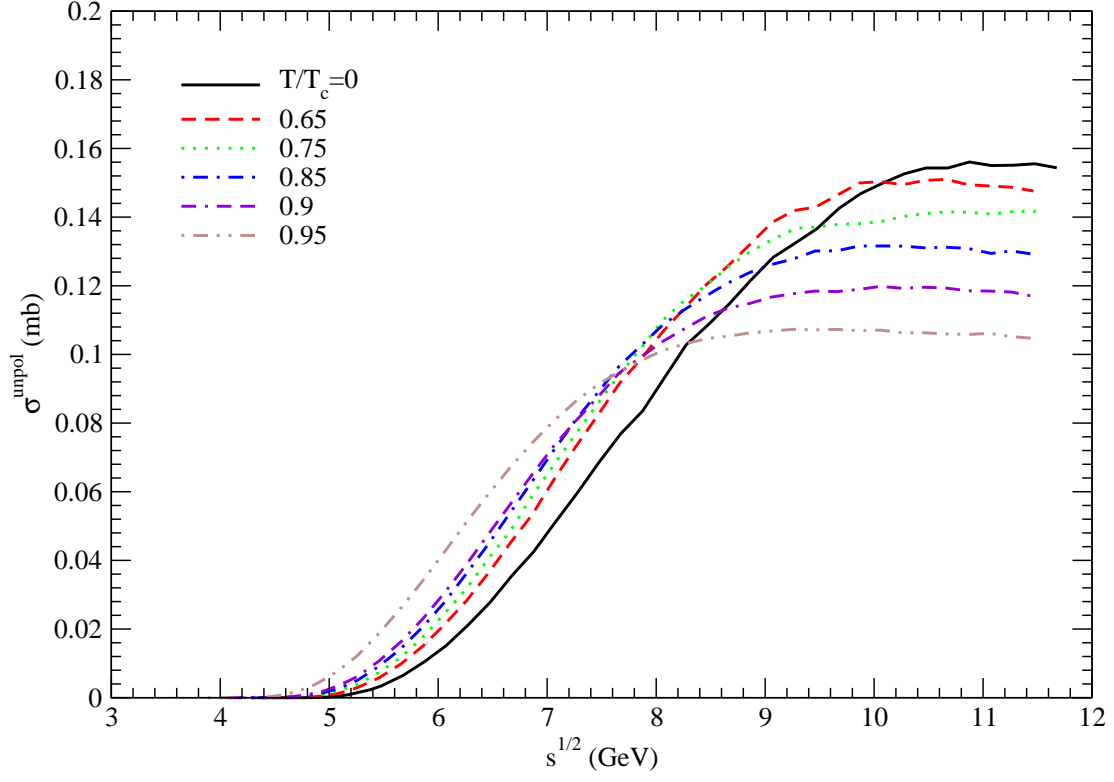


Figure 3: Cross sections for $\pi + J/\psi \rightarrow D_s^+ + X$ at various temperatures.

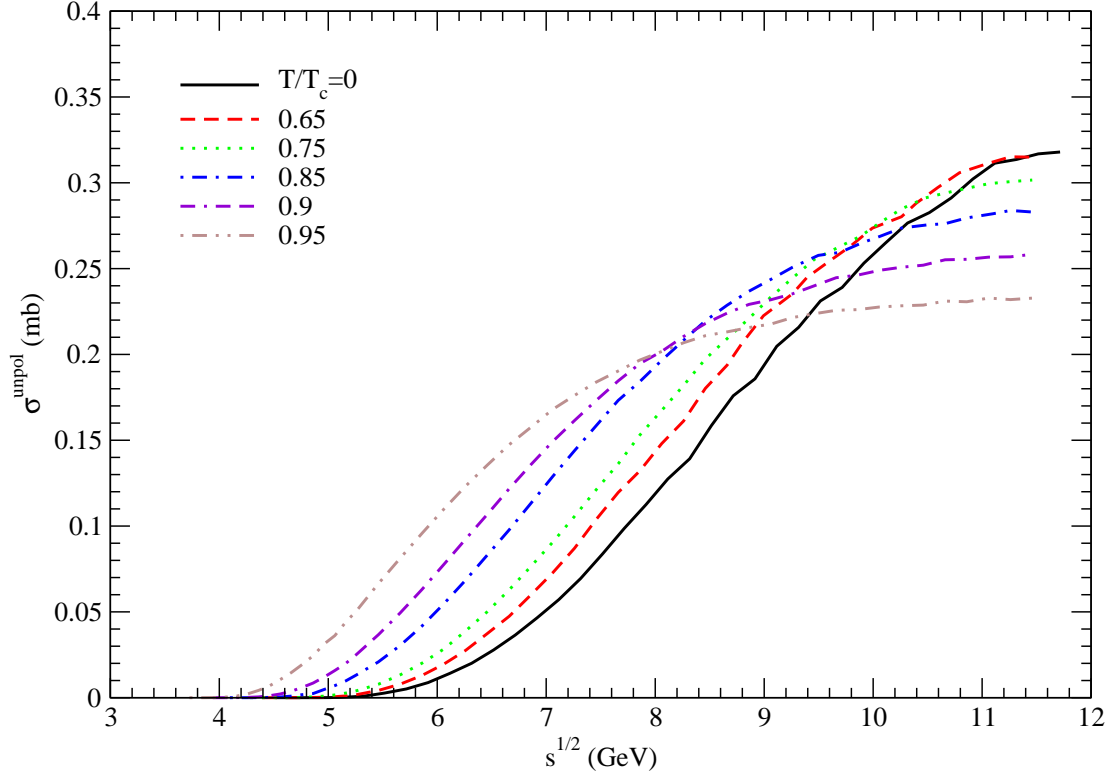


Figure 4: Cross sections for $\pi + J/\psi \rightarrow D^{*+} + X$ at various temperatures.

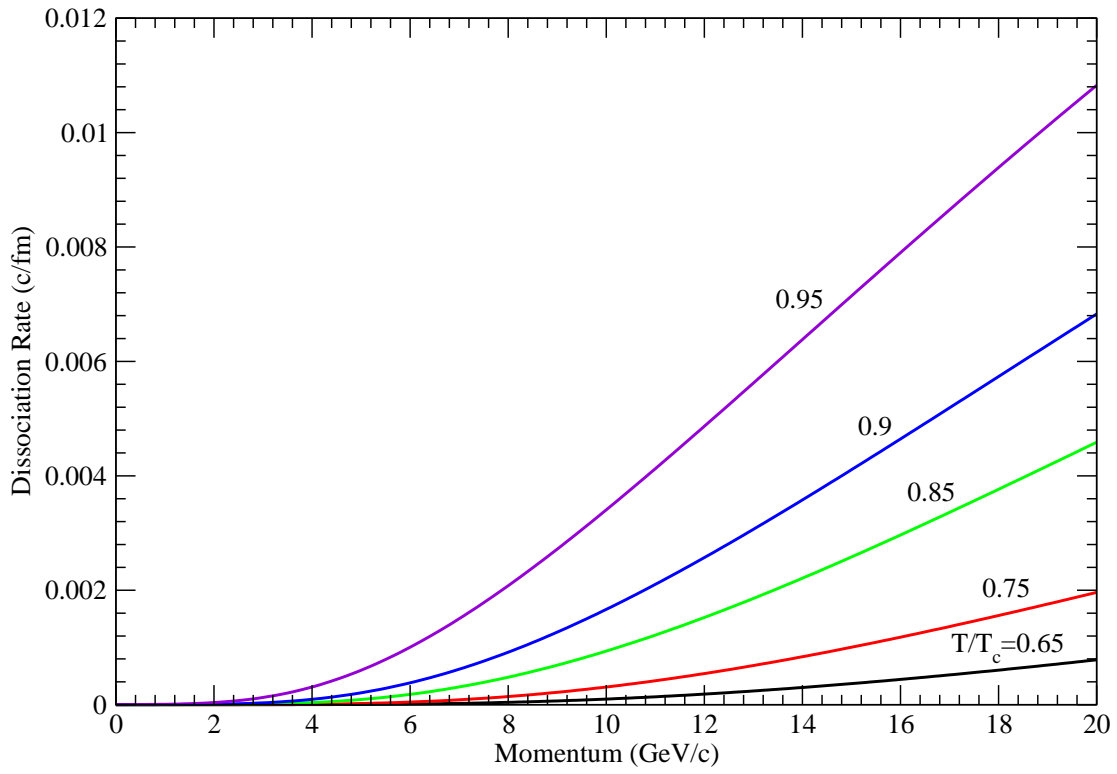


Figure 5: Dissociation rate of J/ψ with π versus J/ψ momentum at various temperatures.

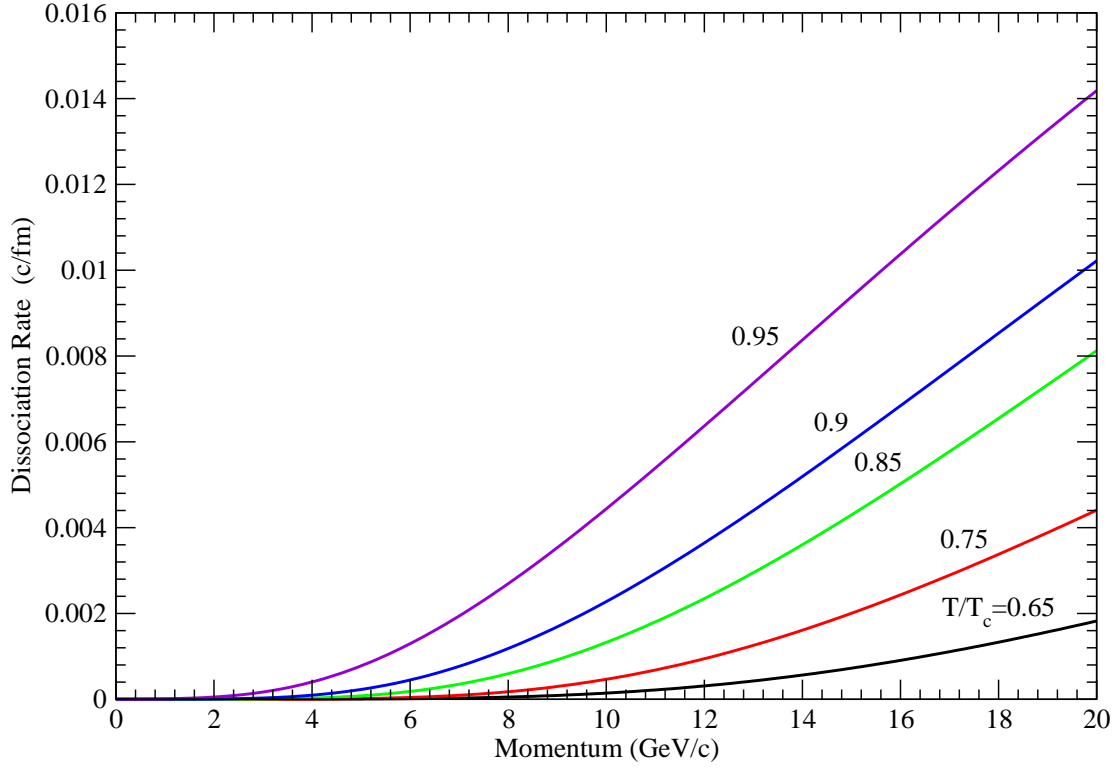


Figure 6: Dissociation rate of ψ' with π versus ψ' momentum at various temperatures.

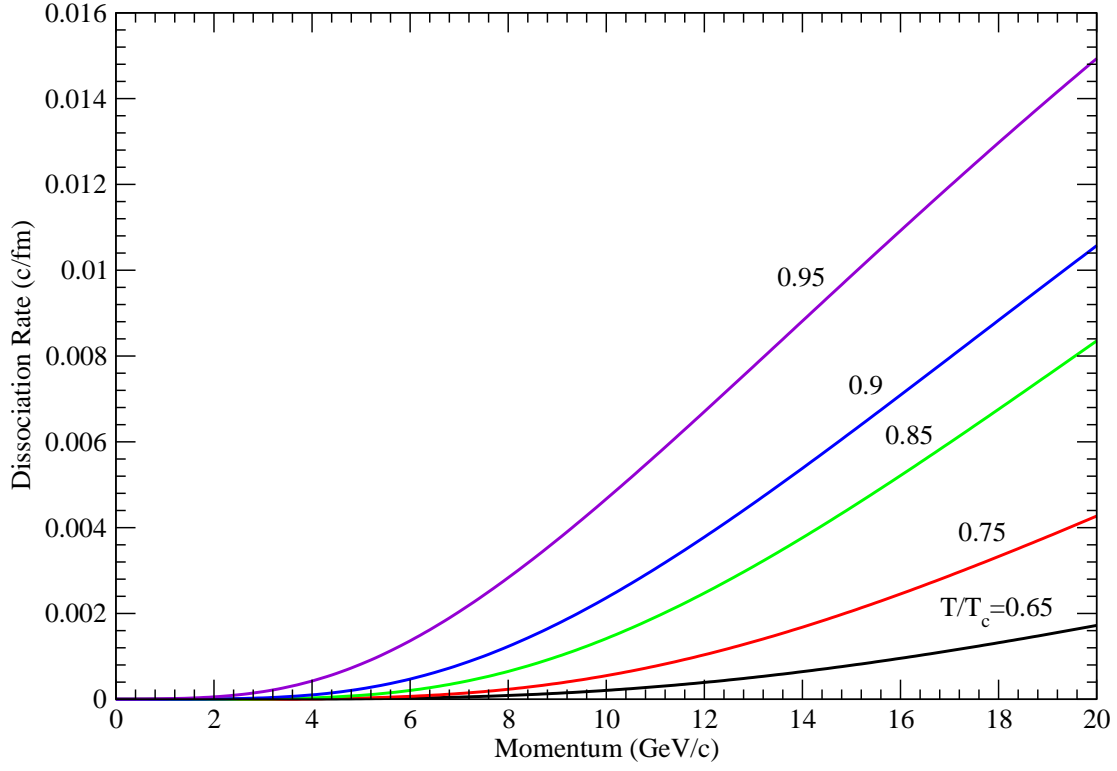


Figure 7: Dissociation rate of χ_c with π versus χ_c momentum at various temperatures.

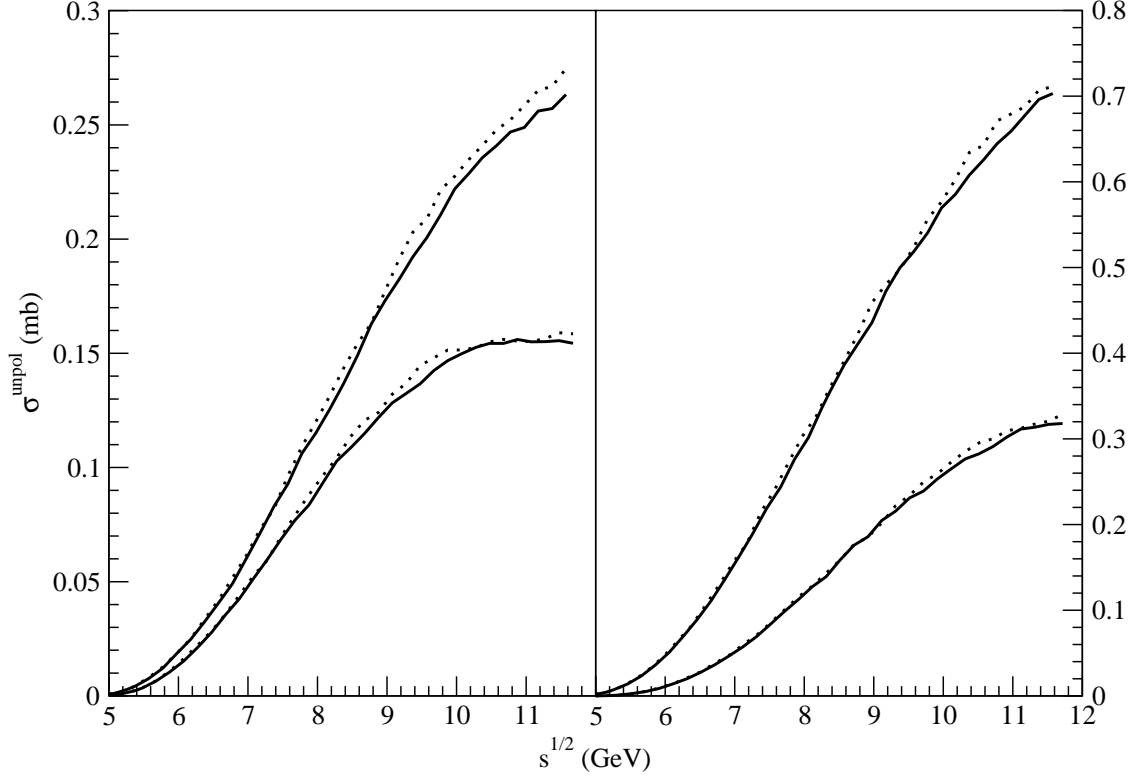


Figure 8: Solid and dotted curves stand for the unpolarized cross sections corresponding to Eqs. (14) and (19), respectively. Left (right) panel: the upper and lower pairs of curves correspond to $\pi + J/\psi \rightarrow D^+ + X$ and $\pi + J/\psi \rightarrow D_s^+ + X$ ($\pi + J/\psi \rightarrow D^0 + X$ and $\pi + J/\psi \rightarrow D^{*+} + X$), respectively.

Table 1: Quantities relevant to the cross sections for the $\pi J/\psi$ dissociation reactions. a_1 and a_2 are in units of mb; b_1 , b_2 , d_0 , and $\sqrt{s_z}$ are in units of GeV; c_1 and c_2 are dimensionless.

Reactions	T/T_c	a_1	b_1	c_1	a_2	b_2	c_2	d_0	$\sqrt{s_z}$
$\pi + J/\psi \rightarrow D^+ + X$	0	0.02	2.8	4.9	0.26	7.4	4.7	7.36	27.43
	0.65	0.01	2.7	4.8	0.26	7.4	4	7.38	29.19
	0.75	0.01	2.5	5.9	0.25	7.3	3.8	7.29	29.39
	0.85	0.021	2.9	4.6	0.24	7.4	3.9	7.33	29.26
	0.9	0.07	3.7	4.1	0.21	8.5	4.6	7.87	30.53
	0.95	0.04	2.7	4.5	0.2	7.2	3.8	7.05	28.54
$\pi + J/\psi \rightarrow D^0 + X$	0	0.015	2.16	6.3	0.69	7.68	3.9	7.68	30.54
	0.65	0.03	2.7	5.2	0.68	7.6	4	7.59	29.86
	0.75	0.06	3.2	4.6	0.67	7.9	4	7.81	30.77
	0.85	0.028	2.5	6.4	0.61	7.2	3.6	7.19	29.59
	0.9	0.064	2.93	4.5	0.57	7.38	3.8	7.27	29.38
	0.95	0.08	2.5	4.7	0.53	6.9	3.9	6.83	27.22
$\pi + J/\psi \rightarrow D_s^+ + X$	0	0.02	3.5	4.7	0.15	6.9	4.1	6.61	27.34
	0.65	0.02	2.7	5.2	0.15	6.1	4.9	5.98	22.99
	0.75	0.05	4	4.5	0.12	7.5	3.9	6.22	29.36
	0.85	0.018	3.1	6.5	0.132	6.2	3.9	5.98	25.25
	0.9	0.04	3.5	5.3	0.11	6.8	4.5	5.93	25.47
	0.95	0.05	3.3	5.3	0.1	7.1	4.9	6.11	25.41
$\pi + J/\psi \rightarrow D^{*+} + X$	0	0.027	3.5	4.9	0.31	7.5	5.3	7.39	26.63
	0.65	0.04	3.3	5.4	0.3	7	6	6.86	23.93
	0.75	0.01	2.6	8	0.31	7.2	4	7.2	28.51
	0.85	0.01	1.7	14	0.29	6.3	3.9	6.3	25.57
	0.9	0.06	3	4.5	0.25	7	4.2	6.67	26.88
	0.95	0.06	2.58	4.5	0.232	6.7	3.8	6.48	26.81

Table 2: The same as Table 1 except for $\pi\psi'$.

Reactions	T/T_c	a_1	b_1	c_1	a_2	b_2	c_2	d_0	$\sqrt{s_z}$
$\pi + \psi' \rightarrow D^+ + X$	0	0.013	1.8	8.9	0.44	6.6	3.9	6.6	26.86
	0.65	0.209	4	13.1	0.76	9.2	4.7	9.18	32.97
	0.75	0.13	3.4	16	0.6	7.3	5.5	7.29	25.4
	0.85	0.11	3.4	9	0.4	7.1	5.5	6.92	24.65
	0.9	0.067	3.2	6.7	0.3	7	4.5	6.78	26.16
	0.95	0.04	2.9	5	0.24	7	3.1	6.78	30.48
$\pi + \psi' \rightarrow D^0 + X$	0	0.03	1.6	15	1.16	6.8	3.8	6.8	27.84
	0.65	0.001	0.7	5	1.8	6	6.8	6	20.21
	0.75	0.7	4.1	11	3.22	14.4	4.1	14.4	52.08
	0.85	0.12	2.9	12.7	1.06	6.3	5.5	6.29	22.35
	0.9	0.13	3	7.5	0.81	6.9	4.4	6.82	26.1
	0.95	0.13	3	4	0.61	6.9	3.9	6.54	27.14
$\pi + \psi' \rightarrow D_s^+ + X$	0	0.012	2.2	8.4	0.27	5.9	3.8	5.9	24.84
	0.65	0.27	3.9	17	0.42	9	4.5	8.99	32.99
	0.75	0.15	3.3	27	0.34	6	6.7	5.98	20.3
	0.85	0.1	3.2	20	0.249	6	6.7	5.95	20.18
	0.9	0.071	3.2	14.5	0.175	6	6.2	5.8	20.6
	0.95	0.06	3.1	8.7	0.13	6.3	4.9	5.7	23.08
$\pi + \psi' \rightarrow D^{*+} + X$	0	0.009	1.7	12.1	0.52	6.8	4.2	6.8	26.87
	0.65	0.4	4.3	18	1.98	14.4	4.4	14.4	50.68
	0.75	0.23	3.8	19	0.73	7.8	6	7.78	26.09
	0.85	0.116	3.1	15	0.5	6.1	5.9	6.05	21.28
	0.9	0.1	2.8	7.4	0.37	6	5.9	5.83	20.81
	0.95	0.12	3.2	4	0.25	7	3.8	5.67	27.55

Table 3: The same as Table 1 except for $\pi\chi_c$.

Reactions	T/T_c	a_1	b_1	c_1	a_2	b_2	c_2	d_0	$\sqrt{s_z}$
$\pi + \chi_c \rightarrow D^+ + X$	0	0.07	3	4.3	0.41	7.6	4.8	7.45	27.8
	0.65	0.03	3.4	14	0.53	7.2	4.2	7.19	27.95
	0.75	0.11	3.8	9.6	0.5	7.7	4.4	7.48	28.92
	0.85	0.12	3.4	7.8	0.39	6.8	6.6	6.51	22.27
	0.9	0.1	3.5	5.7	0.29	7.3	5.2	6.75	25.54
	0.95	0.1	3.7	4	0.25	9.6	3	8.59	40.94
$\pi + \chi_c \rightarrow D^0 + X$	0	0.06	2.3	5	1.04	7.2	3.8	7.19	29.22
	0.65	0.14	4	9	1.39	7.9	4	7.76	30.85
	0.75	0.42	4.1	8.6	1.58	10.1	3.9	10.02	38.6
	0.85	0.2	3.2	8.7	1.05	6.7	5.6	6.59	23.35
	0.9	0.25	3.6	5.9	0.81	8	4.4	7.56	29.57
	0.95	0.12	3	4	0.64	6.8	3.7	6.46	27.41
$\pi + \chi_c \rightarrow D_s^+ + X$	0	0.04	2.6	5.2	0.25	6.5	4.3	6.4	25.59
	0.65	0.1	4.1	7	0.27	6.5	4.5	5.52	24.64
	0.75	0.11	3.5	15	0.3	6.3	5.1	5.89	23.16
	0.85	0.13	3.4	13.3	0.23	6.3	7.5	5.88	20.2
	0.9	0.11	3.4	11.3	0.17	6.4	8.3	5.82	19.7
	0.95	0.065	3	9.9	0.14	6.1	5.6	5.78	21.42
$\pi + \chi_c \rightarrow D^{*+} + X$	0	0.03	2.6	6.1	0.49	7.2	4.5	7.19	27.42
	0.65	0.13	4.4	10.8	0.6	7.8	4.6	7.29	28.87
	0.75	0.2	4.1	12	0.62	8.1	4.8	7.85	29.26
	0.85	0.21	3.5	9	0.47	6.7	7.5	6.25	21.12
	0.9	0.11	3.1	7	0.36	6.6	4.6	6.26	24.66
	0.95	0.13	3.2	4	0.27	7.5	3.7	6.22	29.69

Table 4: Ratio of the difference of the cross sections for $\pi + \psi' \rightarrow H_c + X$ and for $\pi + \chi_c \rightarrow H_c + X$ to the cross section for $\pi + \psi' \rightarrow H_c + X$ at $\sqrt{s} = 9$ GeV.

	$T/T_c = 0.65$	$T/T_c = 0.75$	$T/T_c = 0.85$	$T/T_c = 0.9$	$T/T_c = 0.95$
$D^+ + X$	0.219	0.102	-0.0048	-0.0144	-0.047
$D^0 + X$	0.212	0.103	0.002	-0.014	-0.042
$D_s^+ + X$	0.241	0.107	-0.0063	-0.0183	-0.045
$D^{*+} + X$	0.217	0.108	-0.0103	-0.0136	-0.045
$D^{*0} + X$	0.217	0.108	-0.0103	-0.0136	-0.045